

# Detailed 3D analysis of bolted joints in global shell structures

P. Volgers

*SMR Engineering & Development*

October 2002

## Abstract

This paper summarises the work of SMR performed in the framework of the BOJCAS project [1]. The goal for SMR and CIRA was to be able to perform detailed analysis of bolted joints, including progressive damage modelling, directly embedded into a global structural model. Therefore, several developments were needed in B2000: Contact, a sparse solver and a method for coupling the volume mesh with the shell mesh.

## Contents

<b>1</b>	<b>Introduction</b>	<b>2</b>
<b>2</b>	<b>Sparse solver</b>	<b>2</b>
2.1	Factorisation algorithm . . . . .	3
2.2	Performance . . . . .	3
<b>3</b>	<b>Contact</b>	<b>4</b>
3.1	Contact detection . . . . .	4
3.2	Contact resolution . . . . .	6
<b>4</b>	<b>Shell-volume coupling</b>	<b>8</b>
4.1	Shell to shell connectivity . . . . .	8
4.2	Shell to volume connectivity . . . . .	9
<b>5</b>	<b>Benchmark structure</b>	<b>11</b>
5.1	Modelling . . . . .	11
5.2	Analysis . . . . .	13
<b>6</b>	<b>Conclusions</b>	<b>14</b>

# 1 Introduction

In order to analyse the behaviour of a structure, models of various parts and details need to be created. A model where details are modelled less accurately is called a global model, and a more accurate model is then required to study the local details. An example of a global model is a stiffened panel, where joints are modelled by rigid links or beam elements. The traditional approach of using the input of the results of the global model, usually displacements, as input for the local model is well established and works for most cases, but has two important drawbacks:

- A lack of accuracy in case of non-linearity, either geometrical or material non-linearity.
- No feedback from the local model to the global model.

Therefore, accurate global-local modelling based on the traditional approach of different models can be time consuming.

In the framework of the BOJCAS project, CIRA and SMR proposed and developed a direct coupling method, based on the experience of global-local modelling by CIRA. This method integrates the local model directly into the global model, thereby avoiding the drawbacks mentioned above. The potential disadvantage of the direct coupling, namely increased computation time, is reduced by the use of modern solution techniques and increased computing power by continued developments in processor technology<sup>1</sup>. The coupling of local to global meshes is described in Section 4.

To be able to analyse bolted joints in detail, the B2000 implicit solver has to be able to deal with contact. Therefore the explicit contact search algorithm has been introduced into the implicit code. The contact forces are then solved using the Lagrange-multiplier method. The contact method is described in Section 3.

As both the global and the local models are medium sized, combining them into one model, will create relatively large size problems to be solved. The contact has been implemented in the new sparse matrix solver, which is currently being fully integrated in the B2000 code. This paper starts therefore with a description of this new solver in Section 2.

Finally, Section 5 demonstrates the global-local coupling, including contact around a set of bolts, which has been introduced in a structure from Airbus Deutschland, a stiffened panel with a temporary repair patch.

## 2 Sparse solver

Given the large size of the problems resulting from the detailed analyses and the global-local coupling methods, SMR set out to develop a new solver in the *B2000* code in order to solve these systems in an acceptable amount of time. Part of this work has been performed outside the BOJCAS project. The new solver had to be a direct solution method, given the well-known instability problems of iterative solvers when applied to shell structures. The new solver also had to include the use of Lagrange multipliers for the resolution of certain boundary conditions.

---

<sup>1</sup>Moore's law states that the computing power of CPUs doubles every 18 months. With the duration of the BOJCAS project being 3 years, this means a 4 fold increase between the start and the end of the project.

## 2.1 Factorisation algorithm

The sparse Cholesky factorisation algorithm, as implemented in the *B2000* finite element system, is an adaptation of the Gauss elimination method for symmetric systems, in which only operations on the non-zero entries are performed. This is the major difference from the skyline Cholesky factorisation, which removes only operations on entries outside the skyline.

The basic sparse Cholesky factorisation algorithm is rather straightforward. As an illustration, the right-looking version of the basic sparse Cholesky factorisation of the matrix  $A$  to create the triangular matrix  $L$ , where  $LL^T = A$ , is given below.

1.  $L$  is initialised with  $A$
2. for  $k = 1, n$  do:
3.  $L_{k,k} \leftarrow \sqrt{L_{k,k}}$
4. for  $i \in \text{col}(k)$  do:
5.  $L_{i,k} \leftarrow \frac{L_{i,k}}{L_{k,k}}$
6. for  $j \in \text{col}(k)$  do:
7. for  $i \in \text{col}(k)$  and  $i \leq j$  do:
8.  $L_{i,j} \leftarrow L_{i,j} - L_{i,k}L_{j,k}^t$

Where  $\text{col}(k)$  denotes the set of row indices of sub-diagonal non-zero elements of column  $k$ . However, an efficient implementation of the sparse Cholesky factorisation requires many improvements and the use of complex optimisation techniques. More about these implementations can be found in [2, 3].

## 2.2 Performance

To compare the performance of the old solver (`b2aem` and `b2es`) with the new solver<sup>2</sup> (`b2mes`) a linear analysis of a stiffened panel, including shells and beams (the benchmark structure described in Section 5), has been performed. Table 1 below shows the memory use and timing results for the old assembler and solver, the new solver (with the assembler integrated) with the default renumbering scheme and the new solver using the `Metis` library for the renumbering.

Processor:	Memory use	CPU time (s)	Wall time (min:s)
<code>b2aem</code> and <code>b2es</code>	274 MB	270.3	5:42
<code>b2mes</code> (default)	115 MB	25.0	0:25
<code>b2mes</code> (metis)	105 MB	17.2	0:17

Table 1: Timing and memory use of solvers (*P4 1.8GHz*)

We do not only obtain a large reduction of memory use (40% less), but an enormous improvement of computation time (factor of 10). The traditional assembler requires not only a lot of memory, but is very CPU inefficient, due to many disk accesses. Using the `metis` library for renumbering we gain an additional 30% in computation time.

<sup>2</sup>The new sparse solver makes heavily use of the `blas` library. A good implementation of the `blas` routines, by using the `atlas` library, will improve performance even further.

## 3 Contact

The resolution of the contact problem consists of two parts: The detection of the contact and the computation of the contact forces. Both parts are equally important and time consuming. An effective method of detecting the nodes in contact can greatly reduce the computation time. SMR developed an efficient implementation of the contact search for its explicit solver, which could be used with some minor modifications for the implicit solver.

### 3.1 Contact detection

With the total contact surface divided into contact segments (or contact surface elements), the contact search can be performed in three steps [11]:

1. Slave node sort and global contact surface search by means of a bounding box around the total contact surface.
2. Renewed slave sort on reduced set and bounding box search on each of the contact segments.
3. Computation of the distance of the slave node to the average master segment on a limited set of nodes.

In order to obtain locality of data (for processor efficiency) and to limit the duplication of information and to limit the amount of program code, the contact search has been implemented in C++, making use of advanced features of the standard template library (STL). This resulted in code which requires the use of advanced compilers, but which is very efficient.

In explicit analysis, the contact search is often as time consuming as the computation of the contact forces. Especially when many potential contacting nodes are involved, the contact problem can take up to 50% of the total analysis time, with the time spend on contact evenly split between the contact search and computation of the contact force. An efficient implementation of the contact search will therefore greatly reduce the total analysis time. See [13] for a detailed description of contact algorithms.

Figure 1 shows a general contact problem, with a structure in the middle which can come into contact with two surfaces on each side. The contact definition is based on a master and a slave surface, where the slave surface is not allowed to penetrate the master surface. The force needed to prevent the slave surface from penetrating is also placed as a reaction force on the master surface. A finite element implementation usually defines the slave surface by its nodes and the master surface by its elements or contact segments. This is the so-called node-to-segment contact as implemented in B2000. For this method to function properly, the slave surface is usually the surface with the finer mesh than that of the master surface. Figure 2 shows this finite element discretisation in more detail. The master surface is made of contact segments, while the slave surface is discretised by the slave nodes. The same slave nodes can be defined for multiple master surfaces, or the slave surface of one contact definition can be the master surface for another contact description.

Because contact can occur on only one side of the surface, a outward normal has to be defined. The outside is given by the counter-clockwise numbering of the master contact segments. The contact force is then directed along this normal.

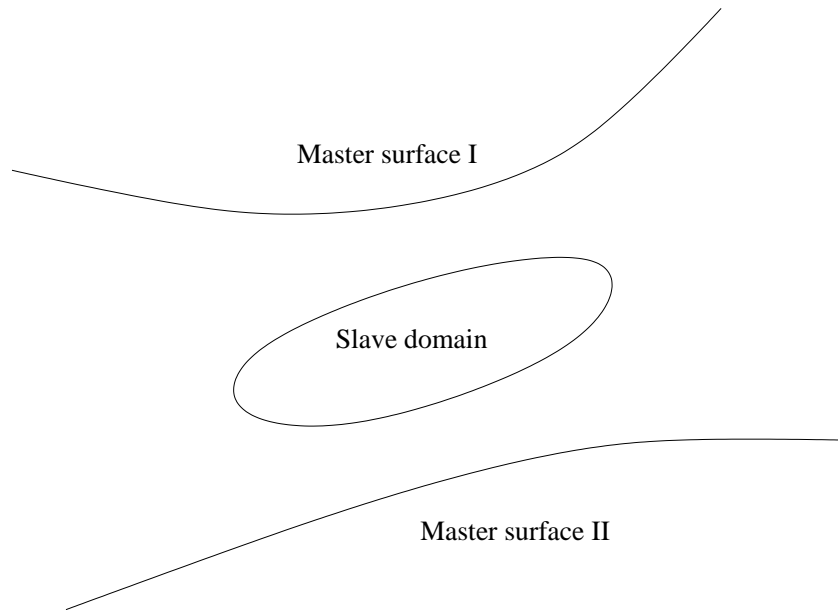


Figure 1: General contact definition: Master and slave

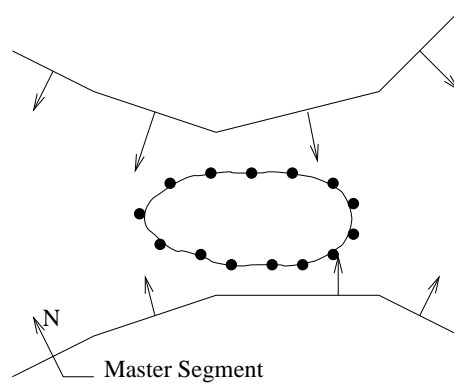


Figure 2: Master segment and slave nodes

### Global surface search

The contact search method implemented in B2000 makes use of a three-stage search, where the two first stages make use of a so-called bounding-box search. This bounding box search is shown in Figure 3. The first phase of the contact search creates a box around the total master surface and searches for all nodes which are inside this surface bounding box. This search is done only initially and after a fixed number of steps or iterations, depending on the displacement of the structure. In practice, this means that in most quasi-static cases the surface box search is performed only once. Any slave node outside this box (e.g. slave node 1) is no longer taken into account during the following analysis.

### Global segment search

On this now (hopefully) limited set of slave nodes the local (i.e. master segment wise) contact search is performed. This local search is done in two steps: First a bounding box search is

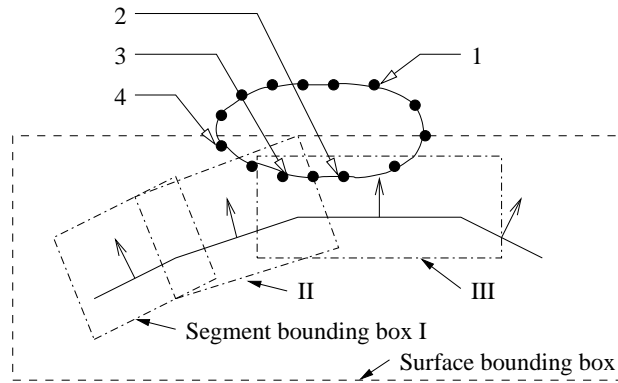


Figure 3: Bounding box search on master surface and master segment

performed, similar to the one on the global surface. This gives for each master segment a set of nodes which have the potential to come into contact with the master segment. Some nodes are found only in the box of one particular segment (e.g. slave node 2), so that this slave node is only considered a potential contacting node for the corresponding master segment (in this case segment III). Other nodes are found to be in the overlap of two or more master segment bounding boxes (e.g. slave node 3). And some nodes are not inside one of the local bounding boxes (e.g. slave node 4), so that they are no longer considered in the analysis until the next local bounding box search. This local search will usually take place more often than the afore mentioned global bounding box search.

### Local segment search

Finally, for each node within the bounding box of the master segment, the projection of the slave node on the master segment is computed. When the projection lies within the surface of the contact segment, the slave node is considered to be in contact with the master segment and is included in the computation of the contact force. A tag is given to this node to indicate it is in contact with a segment to prevent the contact force on it being computed twice (e.g. node 3, see Figure 4a). A certain margin is allowed to prevent nodes falling into a 'contact gap', as shown in Figure 4b.

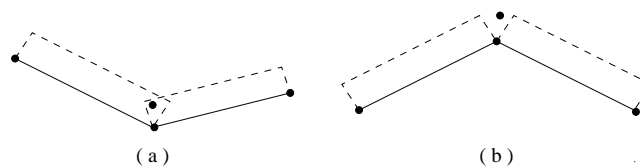


Figure 4: Slave node in a valley (a) or a gap (b)

## 3.2 Contact resolution

The most common method for resolving the contact problem in both static and dynamic analysis is by means of the penalty method. The penalty method itself is known to give results which are highly dependent on the value of the penalty parameter and therefore require expertise in this field of the engineer using the method. The larger the penalty parameter the

less penetration can occur, but a large penalty parameter worsens the condition of the linear system, making it more difficult or even impossible to solve, particularly when iterative methods are being used. Many commercial implementations try to avoid this problem by internally computing an optimum value of this parameter during the simulation. This avoids the problem of requiring experience in choosing the proper penalty parameter by hiding the use of it. However, it means a loss of control over the simulation results and it can result in incorrect answers due to too large penetrations.

A more complex, but better solution, is by making use of the Lagrange multiplier method. The kinematic contact condition for the discrete finite element system can be written as (see e.g. [11, 13]):

$$A_c \mathbf{U} - \mathbf{G} = 0 \quad (1)$$

Where  $A_c$  is the global projection matrix of the slave nodes on the contact surface,  $\mathbf{U}$  the global displacement vector and  $\mathbf{G}$  the corresponding gap vector, denoting the distance between the slave nodes and the contact surface. We now introduce a vector of Lagrange multipliers  $\lambda_i$ , denoted by  $\Lambda$ . The contact force is only non-zero when contact occurs, so that we can combine this into the so-called Kuhn-Tucker condition:

$$\Lambda^T (A_c \mathbf{U} - \mathbf{G}) = 0 \quad (2)$$

The potential energy  $\Pi$  of the discretised system can be augmented by this condition, so that we can write:

$$\Pi(\mathbf{U}, \Lambda) = \frac{1}{2} \mathbf{U}^T K \mathbf{U} - \mathbf{U}^T \mathbf{F} + \Lambda^T (A_c \mathbf{U} - \mathbf{G}) \quad (3)$$

Where  $K$  is the global stiffness matrix and  $\mathbf{F}$  is the global external force vector. This can be solved by variation of  $\Pi$ :  $\delta\Pi = 0$ , or:

$$\left( \frac{\partial \Pi}{\partial \mathbf{U}} \right) \delta \mathbf{U} + \left( \frac{\partial \Pi}{\partial \Lambda} \right) \delta \Lambda = 0 \quad (4)$$

Which must be valid for all variations of  $\delta \mathbf{U}$  and  $\delta \Lambda$ . This yields the following, extended, linear system:

$$\begin{bmatrix} K & A_c \\ A_c^T & 0 \end{bmatrix} \begin{bmatrix} \mathbf{U} \\ \Lambda \end{bmatrix} = \begin{bmatrix} \mathbf{F} \\ \mathbf{G} \end{bmatrix} \quad (5)$$

The resolution of this system gives the exact solution to the contact problem. However, it significantly increases the size of the linear system. The system can become ill-conditioned or even singular, due to possible singularities in the global projection matrix  $A_c$ . This places severe demands on the quality and robustness of the solver and the contact search, as described above.

## 4 Shell-volume coupling

In general, coupling of meshes is a complicated task, which is the topic of current research (see e.g. [6, 7, 8]). In order to be able to apply this to any mesh, multi-node interface elements are developed, which use higher-order polynomials to follow curved edges. However, in aerospace engineering we often work with shell elements and relatively simple geometries. Considering the problems of interest, we can make the following assumptions:

- The global models are thin-walled structures, described by shell theory.
- Use is made of 4 node (linear) shell elements.
- The local model is inserted along a straight line in the plane of the shell.

The first two assumptions allow us to express the connectivity between the course and the fine mesh by means of linear constraints, because the displacement field along the edge of a linear shell element is a linear relation between the two nodes on this edge. The last assumption is in order to facilitate the implementation of the definition of the connectivity. As the work in the BOJCAS project was meant to demonstrate the validity of the integrated model approach for global-local model coupling, this allowed for much faster implementation of the coupling.

### 4.1 Shell to shell connectivity

Connecting two meshes of linear (4-nodes) shells is quite straightforward. Figure 5 shows two meshes with different densities. Because the displacement field between two nodes of an element edge is a linear combination of the displacement  $\mathbf{U}$  of the nodes ( $M^1$  and  $M^2$ ), we can write for the displacements at point  $S$ , placed at a distance  $a$  from node  $M^1$ :

$$\mathbf{U}^s = (1 - a)\mathbf{U}^1 + a\mathbf{U}^2 \quad (6)$$

If the rotations  $\theta$  are expressed in the *global* system, we can write them in a similar way:

$$\theta^s = (1 - a)\theta^1 + a\theta^2 \quad (7)$$

A similar expression can be found when the rotations are expressed in the *local* element frame, except that one should take care of the proper direction of the different local element axes.

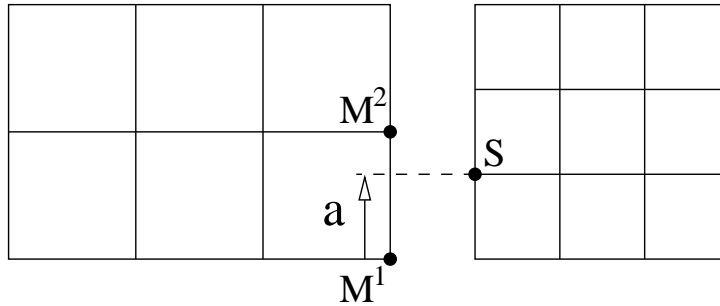


Figure 5: Connecting shell meshes

## 4.2 Shell to volume connectivity

Connecting shell to volume meshes is much more complicated than connecting shell to shell meshes or volume to volume models, as it goes from a three dimensional to a two dimensional description (Figure 6), introducing rotations as additional degrees of freedom to the nodes. Looking at Figure 7 we can find an expression for coupling the degrees of freedom

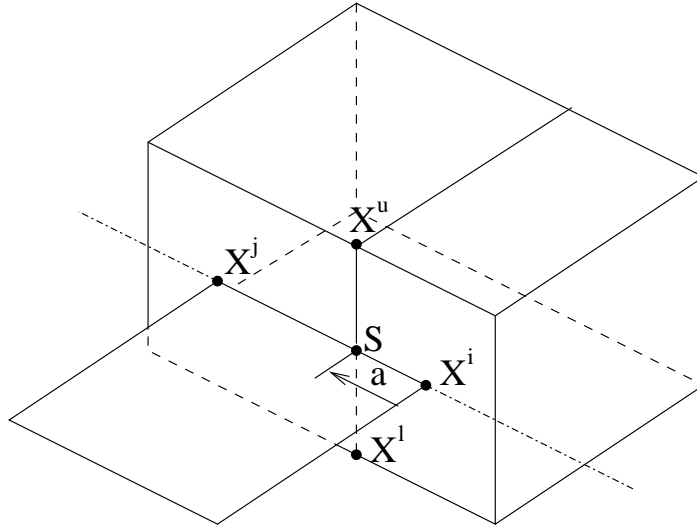


Figure 6: Connecting shell mesh to volume mesh

in the local system. For simplicity we always assume that

- The shell description is the mid-size of the element (no offset)
- The volume mesh is an extension of the shell mesh.
- The volume mesh is regular through the thickness.

If these assumptions are true, then a corresponding set of upper and lower nodes are always at equal distance from the shell. With the distance between the upper and lower nodes of the volume mesh the thickness of the plate, indicated by  $t$ , we can write for the two-dimensional

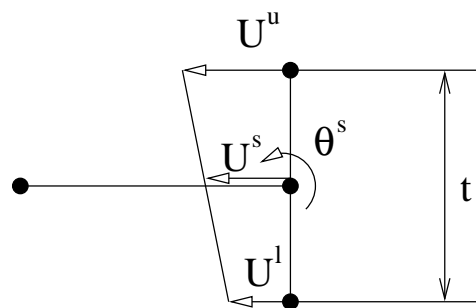


Figure 7: Connecting shell mesh to volume mesh - side view

case:

$$U^s = \frac{1}{2} (U^u + U^l) \quad (8)$$

$$\theta^s = \frac{1}{t} (U^u - U^l) \quad (9)$$

where  $U$  is the horizontal displacement (in the plane of the shell). With  $S$  the intersection of the line  $X^u X^l$  with the edge of the shell element at a distance  $a$  from node  $X^i$ , as shown in Figure 6.

However, expressing the rotation of the shell element in general terms is not a simple task. This would involve constructing the proper element local system, expressing the linear constraints in terms of this local system and then transforming the linear constraints to the global system. This requires the position of the shell element, instead of only the nodal points  $X^i$  and  $X^j$ .

For a quick and simple implementation we assume that the plate is defined in one of the global planes. This will allow us to express the linear constraints directly in terms of the global degrees of freedom. As the goal of the research in the project was to investigate the possibility and usefulness of integrating local detailed models in global models, this was considered to be the most practical approach. If the shell is described in the global  $xy$ -plane, we obtain the following set of linear constraints for a set of nodes of the volume mesh ( $U^u$  and  $U^l$ ), which connecting line intersects the edge of the plate at point  $S$ , placed between the nodes  $X^i$  and  $X^j$  as follows:

$$(1 - a)U_x^i + aU_x^j - \frac{1}{2}(U_x^u + U_x^l) = 0 \quad (10)$$

$$(1 - a)U_y^i + aU_y^j - \frac{1}{2}(U_y^u + U_y^l) = 0 \quad (11)$$

$$(1 - a)U_z^i + aU_z^j - \frac{1}{2}(U_z^u + U_z^l) = 0 \quad (12)$$

$$(1 - a)\theta_x^i + a\theta_x^j + \frac{1}{h}(U_y^u - U_y^l) = 0 \quad (13)$$

$$(1 - a)\theta_y^i + a\theta_y^j - \frac{1}{h}(U_x^u + U_x^l) = 0 \quad (14)$$

where  $h$  is the distance between  $U^u$  and  $U^l$ .

## 5 Benchmark structure

The benchmark structure to be analysed using the global-local coupling method developed by SMR and CIRA was provided by Airbus Deutschland and described in the BOJCAS deliverables D.1.2 and D.2.1-2 [4, 5]. It is based on the temporary repair of the skin in the vertical tail of an Airbus 330/340.

### 5.1 Modelling

The global model was created by the NLR using MSC.Patran and specific PCL-routines from Airbus Deutschland and analysed using MSC.Nastran [12]. The model with its different components is shown in Figure 8. The Nastran bulk data file (BDF) was converted to the B2000 Modelling description language (MDL) file using the conversion tool b2nas.

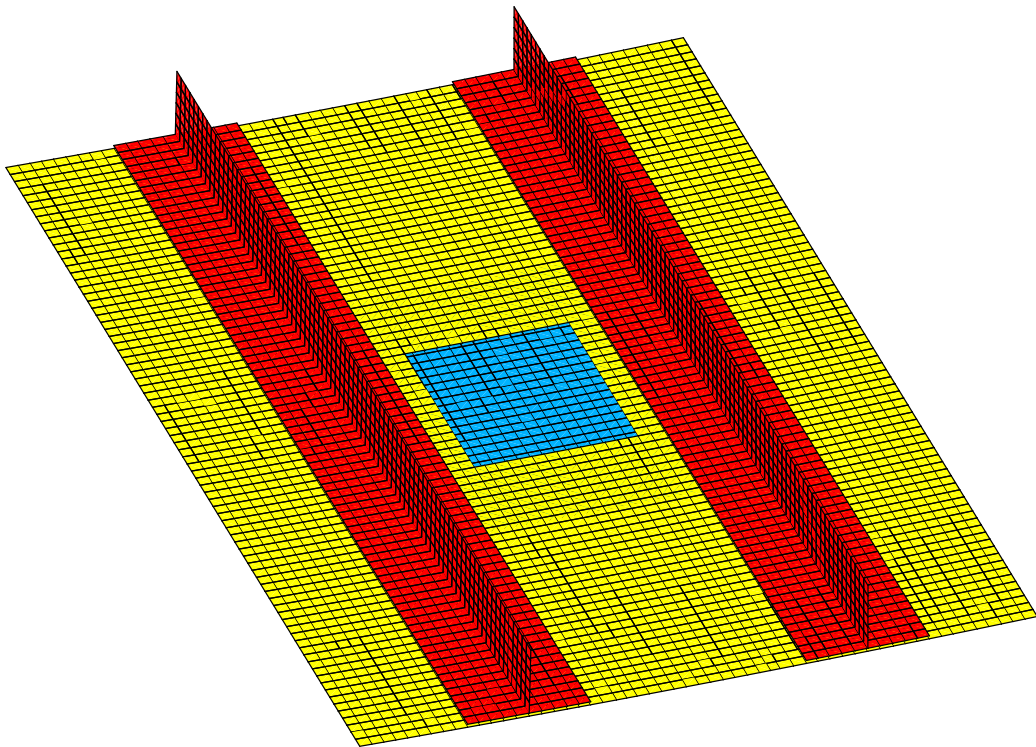


Figure 8: FE model BM-1-T (*converted from Nastran BDF*)

The following components can be seen:

- Skin (yellow).
- Stringers (red)
- Skin patch (light blue)

The structural elements are connected using `rbar` elements. In the B2000 input, they are replaced by beam (`b2`) elements with high stiffness. Results of the analyses of this panel,

both global and global-local model, can be found in the BOJCAS deliverables D4.3-8b and D4.3-8c [9, 10]

A row of three bolts has been replaced by local models. The corresponding beam elements and surrounding shell elements are removed (see Figure 9) to allow the inclusion of the local models.

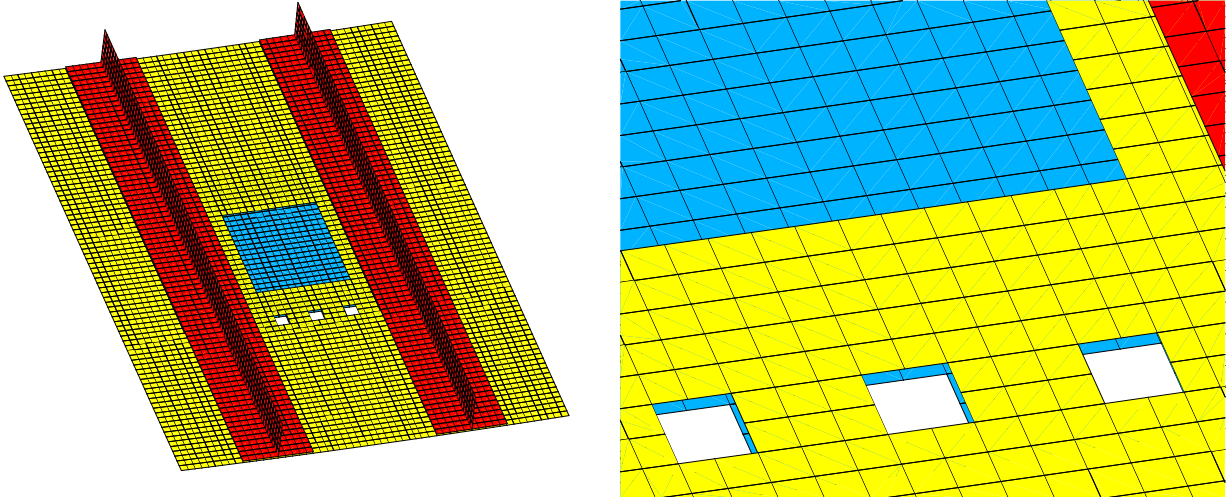


Figure 9: BM-1-T global mesh, elements removed for local model

The local models of the bolts with surrounding plate mesh in 3D are now created and included into the global mesh. Using parametrised input, the same file for the local model can be used for all three 3D meshes. However, the connectivity cannot be parametrised and because no graphical tools for the automatic creation of the connectivity list (both contact and global-local connectivity) were available, this was the most time consuming part of the integration of the local models into the global structure. The result is shown in Figure 10. A newly developed mesh definition input developed later greatly improved the set-up time of the local mesh and the connectivity between the local and the global model.

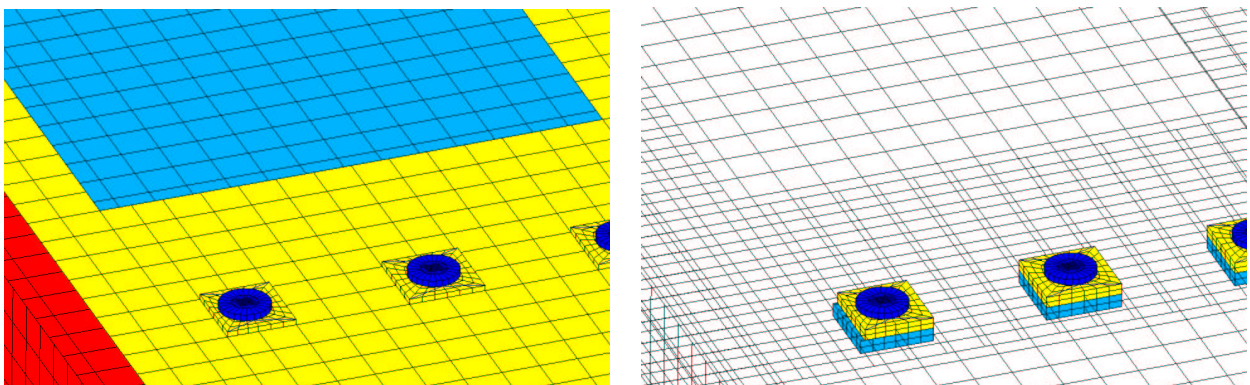


Figure 10: BM-1-T global-local mesh

## 5.2 Analysis

The global-local model is incrementally deformed using force-controlled loading conditions. Figure 11 shows the development of the axial deformation of the global-local model, resulting in a global deformation very similar to the global model.

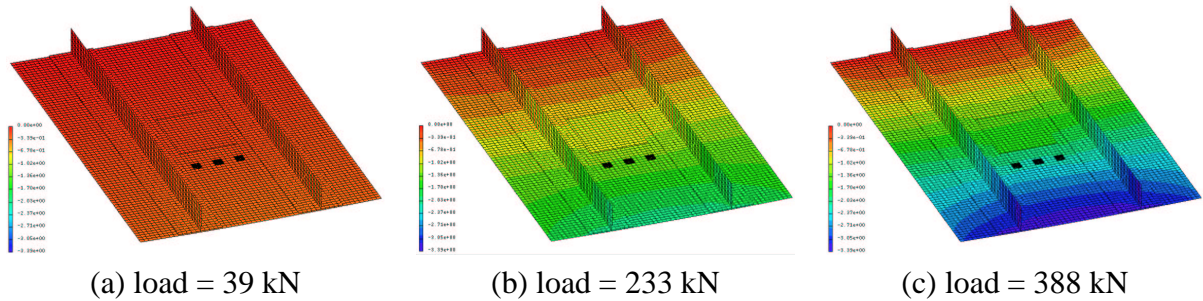


Figure 11: Global-local analysis: axial displacements ( $min/max -3.39/0$ )

Figure 12 shows the development of the out-of-plane displacements, with the creation of a buckling-like pattern. Actual buckling cannot occur in the simulation, as only linear structural analysis has been performed. The contact conditions are the only non-linearity in the modelling.

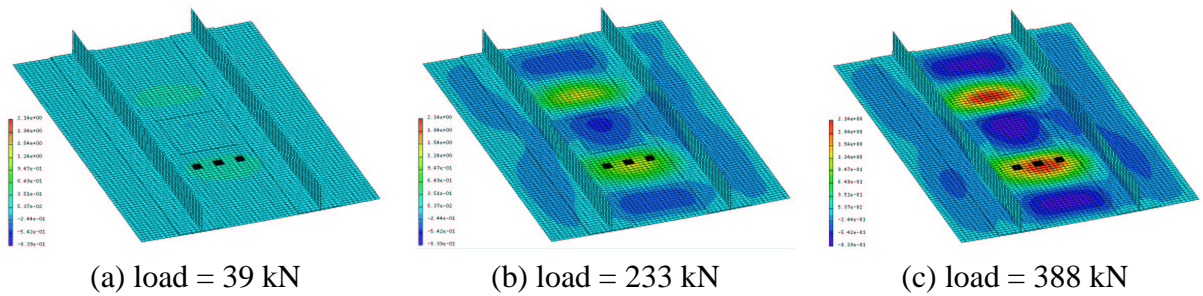


Figure 12: Global-local analysis: out-of-plane displacements ( $min/max -0.84/2.14$ )

The introduction of local models allows for detailed study of the stress situation around the bolt hole. Because the bolt model introduced into the benchmark structure has a small tolerance, this will show up in the post-processor as space between the bolt and the plate, as can be seen in Figure 13(a). The local model allows us to study the load distribution from the plate to the bolt. Figure 13(b) shows the contact load concentration of the patch plate into the bolt.

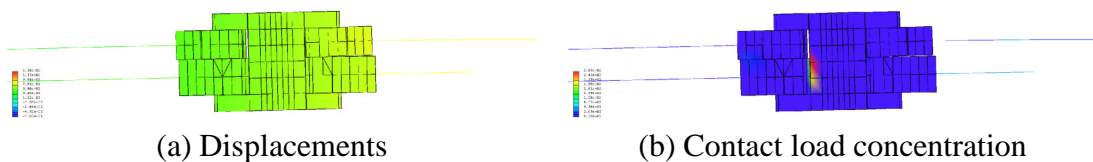


Figure 13: Global-local analysis: results around the bolt. ( $Load: 233\text{ kN}$ )

## 6 Conclusions

This paper gave a summary of the developments by SMR in the framework of the European project BOJCAS. In collaboration with CIRA, SMR introduced a Lagrange multiplier contact method in the sparse solver and a method to couple a global shell mesh with a detailed local volume mesh.

Introducing local detailed models directly in the global model provides the engineer with more and more detailed information about critical aspects of the model. With the computing power we have nowadays on our desktop, the additional computational requirements due to the integrated global-local model, is relatively small. When local behaviour needs to be studied in detail, the global model around the detail provides better boundary conditions and interaction with the rest of the structure, while at the same time hardly increasing the computation time. Most of the time is spent in the resolution of the contact problem, with the solution of the global system (total stiffness matrix) using modern techniques being a fraction of the total solution time.

The Airbus Deutschland benchmark structure of a temporary skin repair was used to evaluate the global-local coupling, whereby a local 3D model of a bolted joint is integrated in the global structural (2D shell) model. This has the advantage of directly applying the correct boundary conditions of the global model into the local model. It also allows for direct more detailed analysis of the joint. The introduction of the local model hardly changes the global behaviour of the structure. Direct global-local coupling is therefore not immediately suited for improving the stiffness behaviour, unless all bolts are replaced by detailed models, which would increase the computation time too much for global design. Local modelling allows for detailed analysis around critical areas and can therefore be used for improved local strength predictions, including full 3D damage modelling.

# Acknowledgements

SMR would like to acknowledge the contribution of the European Commission and the Swiss BBW to the BOJCAS project. We would like to thank all our partners in the project, particularly NLR and Airbus Deutschland for the benchmark structures, CIRA for the collaboration and the University of Limerick for the management.

# References

- [1] BOJCAS. Bolted Joints in Composite Aircraft Structures. Shared-cost RTD project. Competitive and Sustainable growth GROWTH programme, 2000. Contract No. G4RD-CT-1999-00036. Proposal No. GRD1-1999-10216.
- [2] DOREILLE, M. *Athapascan-1: vers un modèle de programmation parallèle adapté au calcul scientifique*. PhD thesis, Institut National Polytechnique de Grenoble, Grenoble, France, 1999. (in french).
- [3] DOREILLE, M. B2SES - a high-performance sparse solver for B2000. In *Proceedings of the 3rd B2000 workshop* (2000). 27-28 November, Enschede, the Netherlands.
- [4] HACHENBERG, D. Definition of DA benchmark joint configurations. Tech. rep., EADS Airbus GmbH, Hamburg, Germany, 2000. BOJCAS Deliverable D1.2.
- [5] JOCHEM, J., AND HACHENBERG, D. Design of DA benchmark joint configurations. Tech. rep., EADS Airbus GmbH, Hamburg, Germany, 2000. BOJCAS Deliverable D2.1-2.
- [6] KRUEGER, R. A shell/3d modelling technique for delaminations in composite laminates. In *Proceedings of the American society for composites* (1999), pp. 843–852. 14th technical conference.
- [7] RANSOM, J. Interface technology for geometrically nonlinear analysis of multiple connected subdomains. In *38th AIAA/ASME/ASCE/AHS/ASC Structures, Structural Dynamics and Materials Conference* (April 7-10 1997), p. 16. FL, AIAA 97-1190.
- [8] RANSON, J., AND KNIGHT JR., N. Global/Local stress analysis of composite panels. *Computers and Structures* 37, 4 (1990), 375–395.
- [9] VOLGERS, P., DOREILLE, M., AND MERAZZI, S. Evaluation of the global-local coupling using the DA benchmark. Tech. rep., SMR, Bienne, Switzerland, 2002. BOJCAS Deliverable D4.3-8b.
- [10] VOLGERS, P., AND VAN RIJN, J. Post-test analysis of benchmark structures DA-BM-1-T and DA-BM-2-P. Tech. rep., SMR, Bienne, Switzerland, 2002. BOJCAS Deliverable D4.3-8c.
- [11] VOLGERS, P. T. G. Contact in finite elements. Master’s thesis, Delft University of Technology, Delft, The Netherlands, 1997.
- [12] WALSHOT, VAN, L., AND RIJN, VAN, J. Global DA benchmark analysis. Tech. rep., NLR, Vollenhove, the Netherlands, 2002. BOJCAS Deliverable D2.2-3.
- [13] ZHONG, Z.-H. *Finite element procedures for contact-impact problems*. Oxford University Press, Walton Street, Oxford, 1993.